# Edge Enhancement Based on an Active Contour Model for the Segmentation of Brain Tumors in MRI Images

**Mustafa Rashid Ismael**, Non-member


## ABSTRACT

Tumor segmentation is one of the most important tasks in brain image analysis due to the significant information contained in the tumor region. Therefore, many methods have been proposed during the last two decades for segmenting tumors in MRI images. In this paper, an automated method is proposed using an active contour model, created using edge sharpening, thresholding, and morphological operations. Four methods of edge detection are utilized in the sharpening process (Sobel, Roberts, Prewitt, and Canny) and their performance investigated in terms of Dice, Jaccard, and F1 score. The experiments implemented on BRATS datasets use both HGG and LGG images. The results of the study indicate that sharpening the edges using detection is essential for improving segmentation of the tumor region, especially when employed with an active contour model. The results demonstrate the effectiveness of the proposed method which outperforms some of the existing techniques.


**Keywords**: Brain Tumor, Edge Detection, Active Contour, Thresholding, Morphological Operations, Image Segmentation

## 1. INTRODUCTION

In computer-aided diagnoses, the segmentation of brain tumors is significant due to the beneficial information obtainable from the tumor region for utilization by radiologists in clinical applications [1]. The segmentation process can be implemented manually or automatically. In manual segmentation, expert radiologists extract the tumor region using their visual experience. The main disadvantages of manual segmentation are the time needed to process MRI slices and the lack of reliability and availability [2]. Besides, manual segmentation relies mainly on the radiologist's decision and results may be different for the same tumor from one expert radiologist to another [3]. Consequently, automatic brain tumor segmentation is necessary for improving the diagnosis process and effective analysis of the tumor region [4]. In automatic brain tumor segmentation, the computer controls the process without any human intervention using soft computing algorithms [5]. Developing a fully automatic system for the segmentation of brain tumors in MRI images can reduce the workload of the physician or radiologist and increase accuracy. However, as a challenging task, it attracts many researchers in different fields such as machine learning, pattern recognition, and medical image processing. In recent decades, many algorithms have been proposed to solve the problem [4]. There are four main methods for brain tumor segmentation: threshold-based, region-based, pixel classification, and model-based [5]. Thresholding is an easy and effective tumor segmentation technique, in which a threshold value is used to separate the image by comparing the intensities of a specific region with that threshold. The threshold value is calculated using either global thresholding [6–8] or local thresholding [9–11]. However, threshold-based segmentation is incapable of employing all the information provided by an MRI.

In region-based segmentation, the image pixel values are utilized to generate different regions by merging homogeneous pixels using a specific rule for similarity. Region growing [12–14] and watershed segmentation [15—19] are both region-based methods [5]. Region-based methods show the lowest degree of accuracy since they are sensitive to noise and require prior knowledge of the anatomical tumor region.

Pixel classification and clustering is another type of segmentation method. In the literature, many algorithms have been suggested, employing clustering techniques, such as fuzzy C-means (FCM) [20], k-means [21], and statistical methods using Markov random fields (MRFs) [22]. Supervised methods include support vector machines [23, 24], artificial neural networks (ANNs) [25, 26], and deep learning [1, 27–29]. The previous classification methods are limited by their inability to process raw data like images. In addition, expert knowledge is required to extract handcrafted features from raw data and convert it into a feature vector from which the input

Manuscript received on April 7, 2021 ; revised on June 24, 2021 ; accepted on July 27, 2021. This paper was recommended by Associate Editor Piya Kovintavewat.

The author is with the Department of Electrical Engineering, University of Babylon, Babel, Iraq.

Corresponding author: eng.mustafa.rashid@uobabylon.edu.iq



Digital Object Identifier 10.37936/ecti-eec.2021193.244942

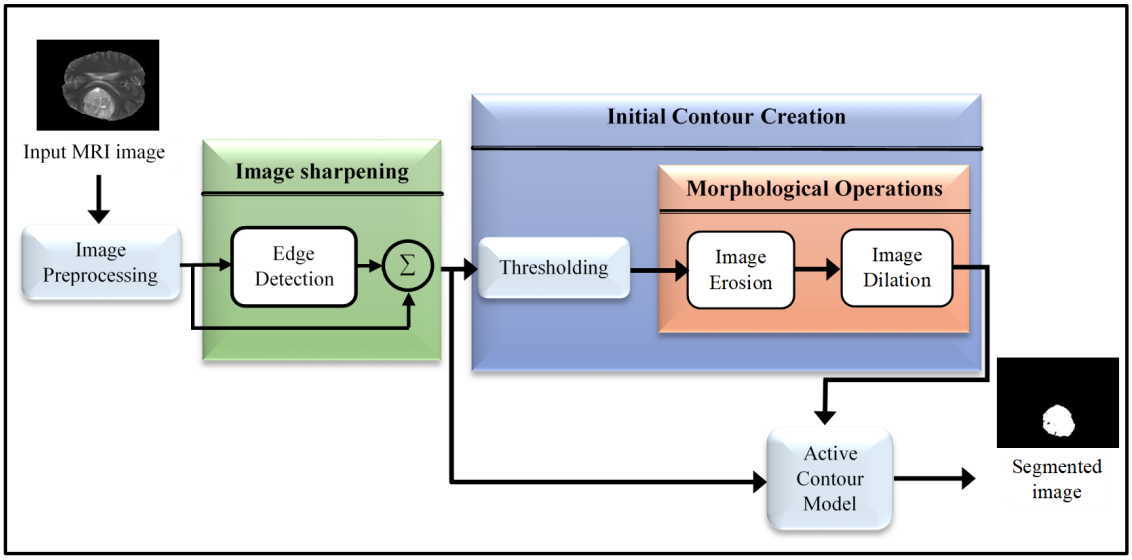


***Fig. 1:*** *Block diagram of the proposed system for tumor segmentation.*

patterns can be classified.

In model-based segmentation, a connected model is constructed by integrating prior knowledge of the object such as its shape, location, and orientation. Deformable models are an example of model-based segmentation, and can be divided into two categories: parametric (active contour models or snakes) and geometric or level sets [5]. Deformable models take advantage of the features associated with region or edge detection in the images. Regional characteristics along with the largest gradients can be exploited to find the tumor boundary. An active contour is an example of a deformable model for tumor segmentation. Different algorithms have been suggested for performing the segmentation process. A fluid vector flow model solves the problem of inadequate convergence in concavities [30]; a content-based active contour utilizes the intensity and texture information to capture a large region in the image [31]. A localized active contour model incorporating the additional step of background intensity compensation is proposed by [32]. An active contour neighborhood-based graph cuts model is suggested by [33] to solve problems such as boundary leakage, over-smoothness, local convergence, and asymmetry. In [34] a local region-based active contour method is suggested to introduce segmentation using the Bayesian framework and a priori information into the data energy term to improve the robustness of noisy image segmentation. Although the model-based techniques present highly accurate and fully automatic segmentation, they suffer from expensive computation.

In this paper, a new algorithm is suggested for segmenting tumors in MRI images using a combination of edge detection, thresholding, morphological operation, and active contour techniques. Firstly, image sharpening is performed by adding the denoised image to one with edges only. Secondly, a mask is created from the sharpened image using thresholding and morphological operations. Finally, the generated mask along the sharpened image is applied to the active contour model to obtain the segmented image. The remainder of this paper is organized as follows: Section 2 presents the methods used to create this algorithm, while the experimental setup is explained in Section 3. Section 4 discusses the simulated results and Section 5 presents the conclusion.

## 2. METHOD

To address the problem of brain tumor segmentation, an active contour model combined with the morphological operation is introduced in this paper. Fig. 1 illustrates the framework of the proposed method.

### 2.1 Preprocessing

To enhance the quality of the MRI images and improve the signal-to-noise ratio, a median filter is applied to the images as a preprocessing step. This filter is designed using a square window in a variable size. In the median filter algorithm, the value of the central pixel in the scan window is changed to the median value of all pixels inside the window after sorting their values [35].

### 2.2 Edge Detection

The edge of an image refers to the borderline between two different regions with two or more levels of intensity represented as gray level. Derivatives (first and second) are frequently used to detect these edges. In image processing, the first derivative is

determined in terms of gradient. The gradient of an image $I(x, y)$ can be written as in Eq. (1) [16].

$$\nabla I = \frac{Fx}{Fy} = \frac{\partial I/\partial x}{\partial I/\partial y}. \tag{1}$$

To obtain sharp edges, the image with edges only is added to the original as shown in Fig. 1. In this algorithm, four types of edge detectors are utilized to sharpen the brain image: Sobel, Roberts, Prewitt, and Canny.

#### 2.2.1 Sobel Edge Detection

The Sobel detection technique employs the edge gradient to find the edges using horizontal and vertical masks, whereby one mask is the transpose of the other [36]:

$$M_x = \begin{bmatrix} -1 & -2 & -1 \\ 0 & 0 & 0 \\ 1 & 2 & 1 \end{bmatrix}, \quad M_y = \begin{bmatrix} -1 & 0 & 1 \\ -2 & 0 & 2 \\ -1 & 0 & 1 \end{bmatrix} \tag{2}$$

where $M_x$ is the horizontal mask and $M_y$ is the vertical mask. The processed image is scanned from left to right and top to bottom using $M_x$ and $M_y$ separately through a convolution process. A sub-window of the image is convolved with $M_x$ and $M_y$ to generate the horizontal gradient $F_x$ and the vertical gradient $F_y$ of the central pixel, respectively. To ascertain whether or not the central pixel is an edge, its gradient is compared with a threshold value. The central pixel is regarded as an edge pixel if the gradient is greater than the threshold value, otherwise, it is a non-edge pixel.

#### 2.2.2 Roberts Edge Detection

The Roberts cross operator implements a simple approximation to the gradient magnitude using two convolution masks [37]:

$$M_x = \begin{bmatrix} -2 & -1 \\ 0 & 0 \end{bmatrix}, \quad M_y = \begin{bmatrix} -1 & 1 \\ -1 & 1 \end{bmatrix}. \tag{3}$$

Therefore, its edge regions are determined according to their high spatial frequency. Each pixel in the input image is represented as its absolute magnitude gradient to make the corresponding pixel in the output image [6].

#### 2.2.3 Prewitt Operator

The Prewitt operator is a discrete gradient method that has two masks convolved with the original image to obtain approximations of the derivatives; one for the horizontal ($M_x$), and the other for the vertical ($M_y$) [38]:

$$M_x = \begin{bmatrix} 1 & 0 & -1 \\ 1 & 0 & -1 \\ 1 & 0 & -1 \end{bmatrix}, \quad M_y = \begin{bmatrix} 1 & 1 & 1 \\ 0 & 0 & 0 \\ -1 & -1 & -1 \end{bmatrix}. \tag{4}$$

#### 2.2.4 Canny Edge Detector

This technique uses a multi-stage algorithm to detect a wide range of image edges. It is useful in finding edges by removing noise from the image, without affecting the edges of the original [6].

The following steps summarize the Canny edge detection algorithm [37, 39]:

1. The image is convolved with a Gaussian function to obtain a smooth image.
2. A finite-difference approximation is performed to obtain the gradient (magnitude and orientation).
3. A double thresholding algorithm is applied to detect the edges, implementing nonmaximal suppression on the magnitude of the gradient.

### 2.3 Thresholding

In image segmentation, thresholding is beneficial for separating the foreground from the background by converting a gray level into a binary image using an appropriate threshold value. With thresholding, the foreground reveals the most significant image information contained in the object of interest. The resultant binary image is constructed by setting all gray level pixels below the threshold value to zero (black), and those above the threshold value to one (white) [40].

### 2.4 Morphological Operation

Two fundamental operations are involved in the implementation of morphological image processing: erosion and dilation. These operations utilize a structuring element and are defined in terms of set notation. In morphological image processing, the erosion operation shrinks the object of interest in the binary image using a predefined structural element, while the dilation operation expands that object [7, 41].

### 2.5 Active Contour Model

Active contours are the most widely used deformable models in image segmentation. In this model, the image domain is deformed to minimize the energy and capture the salient characteristics governed by specified constraints [42]. The snake is an active contour model that is subject to external constraints and controlled by image forces pulling it toward certain features such as lines and edges [43, 44]. A snake model is represented as a direct parametric curve expressed as $(v(s) = [x(s), y(s)], s \in [0, 1])$, where the number of nodes $v(s)$ is referred to as a snaxel and $(s)$ is the normalized arc length in the range $0 < s < 1$. A snake model can be divided into internal and external energy as expressed in Eq. (2) [30, 42, 43, 45]:

$$E_T = \int_0^1 \left[a \cdot E_1\left(v\left(s\right)\right) + b \cdot E_2\left(v\left(s\right)\right) + c \cdot E_3\left(v\left(s\right)\right)\right] ds. \tag{5}$$

The first two terms in Eq. (2) are internal energy, the function of which is to manage the tension and hardness of the snake. The third term is the external energy that attracts the snake to the target contour. The coefficients ($a$, $b$, and $c$) are weighting factors that regulate the significance of the elastic energy ($E_1$), bending energy ($E_2$), and image forces ($E_3$), respectively [46]. The internal energy is constituted from two forces: elasticity and bending, determined as in Eq. (3) [42]:

$$E_{int} = \frac{\left[a\left(s\right)\left|\frac{dv\left(s\right)}{ds}\right|^2 + b\left(s\right)\left|\frac{dv\left(s\right)^2}{ds^2}\right|^2\right]}{2}. \tag{6}$$

The elastic force controls the tension of the snake and is responsible for the stretching and shrinking of the snake contour. Furthermore, the bending force controls the curvature of the snake without changing its length and keeps a smooth curve during the deformation process. In contrast, the external energy is an image-driven force that attracts the snake to the target contour, calculated as in Eq. (4) [42, 43]:

$$E_3 = -c\left(s\right) \cdot \left|\nabla\left(G_\delta\left(s\right)\right) * I\left(s\right)\right|^2 \tag{7}$$

where $\nabla$ is the gradient operator, $I(s)$ is the intensity of the image at $s$, and $G_\delta\left(s\right)$ is the 2-D Gaussian function with a standard deviation $\delta$. The weight function $c(s)$ is usually implemented to control the image coercion [42].

Generally, snake algorithms are performed in three main stages: initialization, deformation, and termination. During initialization, an initial contour around the border of the target object is specified, while the set of weighting parameters $a$, $b$, and $c$ are suitably selected to help the snake deform itself toward the true object boundaries. In the deformation stage, the goal is to minimize the energy function given in Eq. (2) by using the self-deformation implemented in each iteration. Each snaxel (number of nodes $v(s)$) searches for a new location so that it moves toward a pixel with low energy, otherwise it remains in the same location. At each iteration, the total energies are determined by a snaxel and its eight neighboring pixels. When the low energy configuration is achieved, a snaxel moves toward one of the eight possible neighboring pixels, otherwise, it remains in the same location. Finally, the termination stage stops the deformation process due to the snaxels failing to find new appropriate locations. The termination step is essential in the case of snaxel oscillation or boundary shifting that results in an infinite loop, thus a setup involving a maximum number of iterations must be executed during this stage [42].

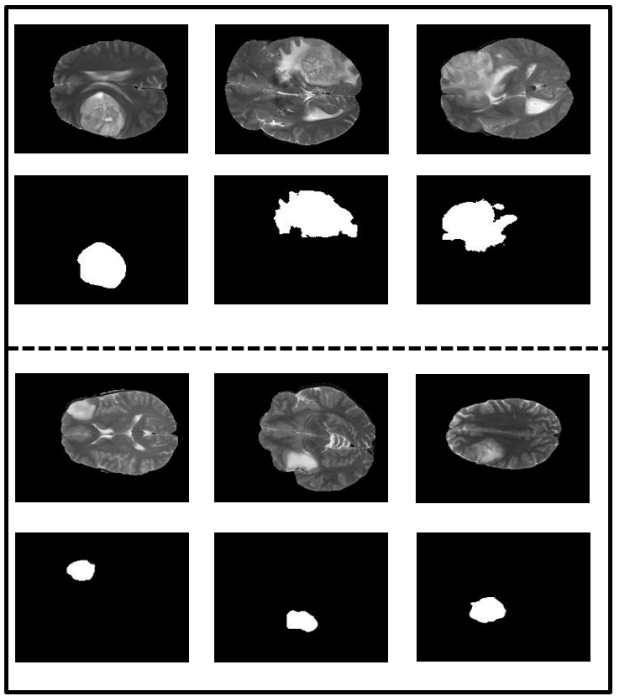

***Fig. 2:*** *Sample images from the BRATS dataset along with its manual expert segmentation (ground truth), upper part HGG images, and lower part LGG images.*

## 3. EXPERIMENTAL SETUP

The proposed algorithm includes image sharpening using edge detection, initial contour creation employing thresholding and morphological operations, and segmentation of the tumor area by an active contour model. The brain tumor image used in this algorithm was obtained from the Multimodal Brain Tumor Segmentation Challenge [4].

This dataset consists of 220 brain images of patients with a high-grade glioma (HGG) tumor and 54 brain images of patients with a low-grade glioma (LGG) tumor. A few examples of these HGG and LGG images are depicted in Fig. 2.

In the preprocessing step, a median filter with a window size of 5 was used for denoising purposes. To improve the sharpness, an image with edges only is added to the denoised image using four methods of edge detection: Sobel, Roberts, Prewitt, and Canny. An active contour with a snake model is initialized close to the object of interest (the tumor region in this algorithm). This initialization is achieved by using thresholding and morphological operations to create an approximated tumor region for employment in the snake model.

In this algorithm, the tumor segmentation performance in MRI images is measured in terms of three

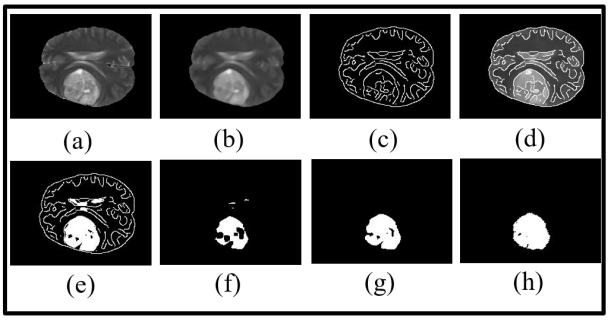


***Fig. 3:*** *Segmentation process, (a) original image, (b) denoised image, (c) image with edges only, (d) additional images in (a) and (c), (e) binary image, (f) eroded image, (g) dilated image, and (h) segmented image.*

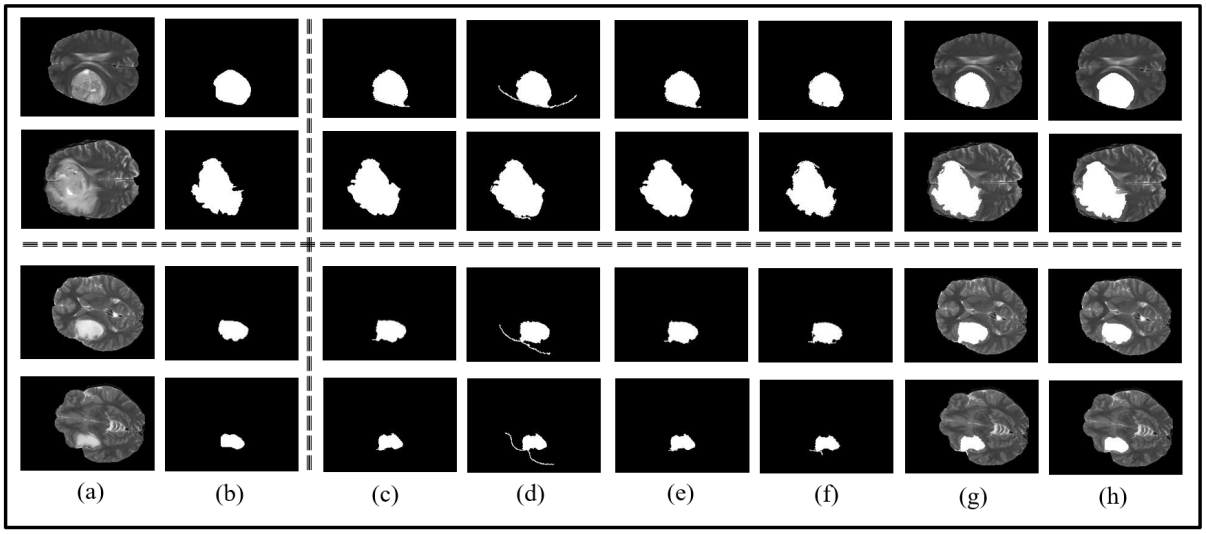


***Fig. 4:*** *Segmentation results using edge detection techniques, (a) original image, (b) ground truth, (c)–(f) segmentation using Sobel, Roberts, Prewitt, and Canny, respectively, (g) overlay of the proposed segmented region on the brain image, (h) overlay of the ground truth on the brain image (the upper two rows refer to the HGG images, while the lower two rows represent the LGG images).*

similarity coefficients, Dice, Jaccard, and F1 score. Given two sets of pixels in the binary images A and B, the ground truth (from the database) is denoted as A while the segmented image is denoted as B. Using the proposed method, the Dice, Jaccard, and F1 score are calculated as in Eq. (8)–(10) [47, 48]:

$$\text{Dice} = \frac{2\,|A \cap B|}{|A| + |B|} \tag{8}$$

$$\text{Jaccard} = \frac{|A \cap B|}{|A \cup B|} \tag{9}$$

$$\text{F1 score} = \frac{2 * \text{precision} * \text{recall}}{\text{recall} + \text{precision}} \tag{10}$$

where $\text{precision} = \dfrac{|A \cap B|}{|B|}$ and $\text{recall} = \dfrac{|A \cap B|}{|A|}$.

## 4. RESULTS AND DISCUSSION

In this section, the results of the proposed segmentation method are presented and compared both qualitatively and quantitatively. Fig. 3 presents the segmentation process, implemented using different methods. The proposed segmentation process is applied in five stages: image preprocessing, edge detection, thresholding, morphological operations, and active contouring. In the image preprocessing stage, a median filter is utilized as a denoising method for enhancing the image and reducing the noise. The Canny operator is used in the edge detection stage as shown in Fig. 3, while a global threshold is used to convert the gray image into a binary image after adding the edges to the denoised image. Two morphological operations are carried out to remove the non-tumor regions and create an initial contour to be utilized by an active contour model for producing the segmented tumor area.

For a visual comparison of the various edge detection methods, the texture results are presented in Fig. 4. Four samples of brain slices (two HGG and two LGG images) are segmented using the prescribed

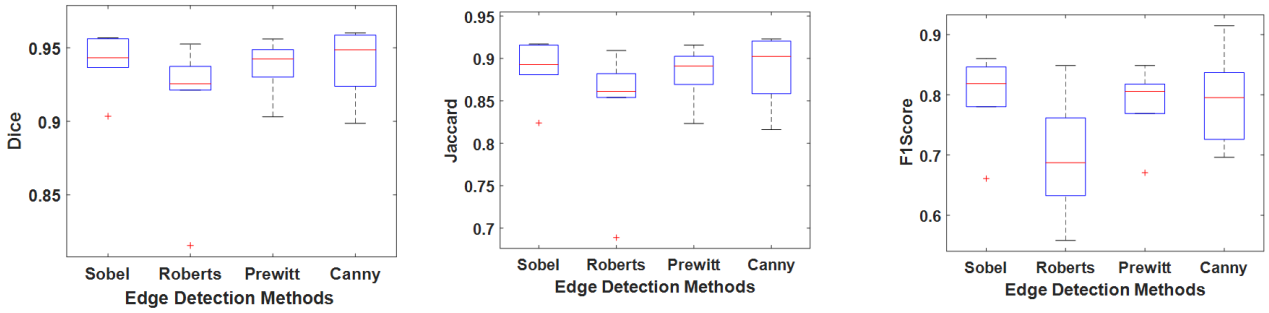


***Fig. 5:*** *Performance of the edge detection methods in terms of Dice, Jaccard, and F1 score on HGG images using boxplots.*

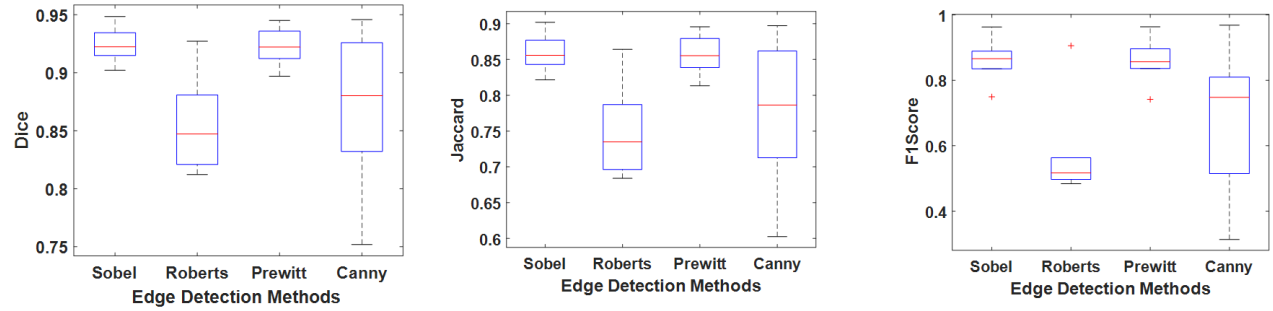


***Fig. 6:*** *Performance of the edge detection methods in terms of Dice, Jaccard, and F1 Score on LGG images using boxplots.*

four detection methods. Some parts of the tumor are mistakenly segmented as healthy tissue using Roberts and Prewitt techniques, while on the other hand, some parts of the healthy tissue are segmented as a tumor. Convenient approximation to the ground truth tumor is obtained using Sobel and Canny edge detection methods.

Fig. 5 shows a quantitative comparison of the edge detection methods for HGG brain images in terms of Dice, Jaccard, and F1 score. As it can be observed, Sobel and Canny exhibit the best performance compared to Roberts and Prewitt methods. On the other hand, Fig. 6 shows a quantitative comparison of the edge detection methods for LGG brain images in terms of Dice, Jaccard, and F1 score.

Sobel and Prewitt methods performed better than Roberts and Canny. As stated in Section 2.2, the edges in an image can be produced using methods such as Sobel, Roberts, Prewitt, and Canny. However, the performance of the segmentation depends on the original image. During edge detection, false edge fragments are created due to the many levels of intensity gradation in the image after the enhancement process.

For the two grades of MRI brain images (HGG and LGG), the performance of the proposed algorithm is compared using the two methods. In the first method, brain tumor segmentation is conducted in three stages: image sharpening, global thresholding, and morphological operations [49]. In the second method, an active contour model is generated for segmentation with the aid of an initial contour created using thresholding and morphological operations [50]. Figs. 7 and 8 present a comparison between the proposed algorithm and previous methods. As mentioned in Section 2.5, active contours are widely used in image segmentation to minimize energy and capture the salient characteristics of the image. Besides, edge sharpening using edge detection methods improves the segmentation process and reduces the false negatives and false positives by emphasizing the tumor border. The limitation of method 1 is that the generated tumor segment lacks the powerful maximization technique offered by the snake model while method 2 suffers from the absence of sharp edges which are beneficial in generating an initial mask of a tumor. As a result, the proposed algorithm shows better performance in terms of Dice, Jaccard, and F1 score for both HGG and LGG images.

A preprocessing stage is implemented prior to edge detection. The median filter increases the performance of the segmentation process by reducing the noise level in the image and enhancing its visual appearance. Samples of the results are presented in Fig. 9 to prove the beneficial effect of the median filter performance. It can be concluded from Fig. 9 that applying image denoising in the preprocessing step achieves a better performance compared to without

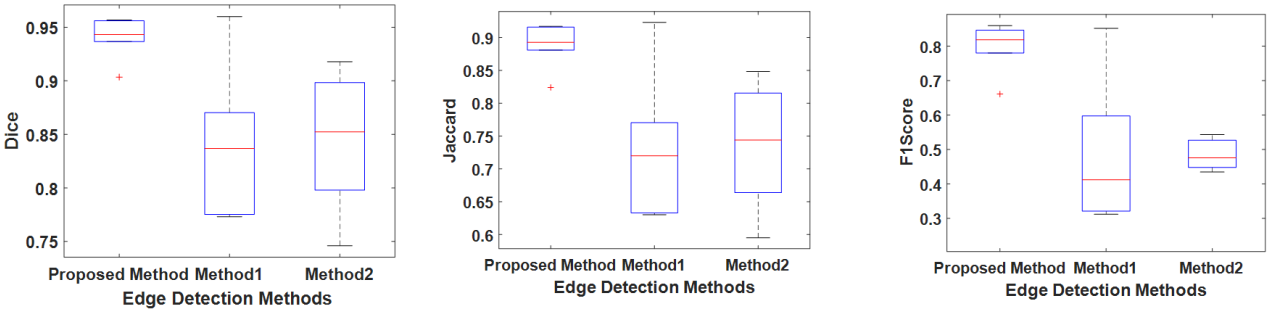


***Fig. 7:*** *Comparison between the proposed method and the two segmentation methods applied to HGG images.*

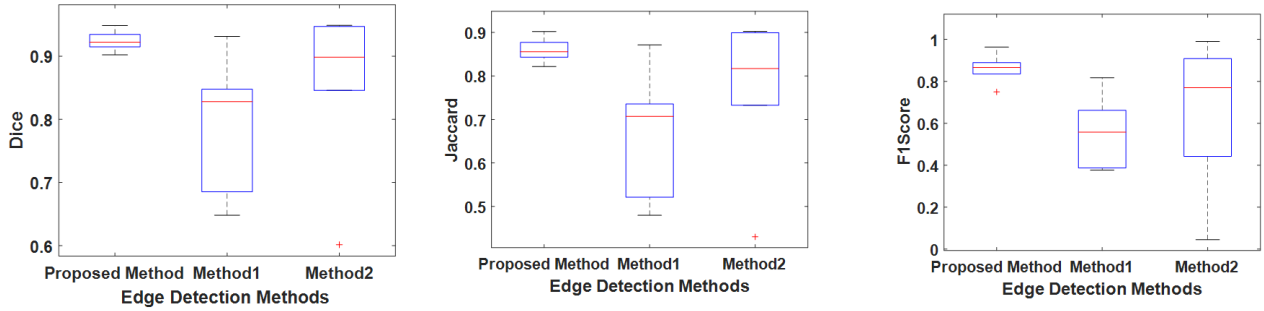


***Fig. 8:*** *Comparison between the proposed method and the two segmentation methods applied to LGG image.*


***Fig. 9:*** *Preprocessing median filter performance (a) HGG Images and (b) LGG Images.*

the denoising process.

Table 1 shows a comparison between the proposed method and those used in recent research methods. The comparison indicates that the proposed method in this study outperforms the existing methods to the best of the researcher's knowledge, for the following reasons.

Segmentation based on pixel classification is implemented using a discriminative or pattern recognition model. Such models require a large number of training samples to ensure robustness against the artifacts in the training images like intensity and shape variations. Furthermore, they are limited by

***Table 1:*** *Performance comparison between the proposed algorithm and state-of-the-art methods.*

| Algorithm | Dice coefficient | |
|---|---|---|
| | LGG | HGG |
| Hierarchical regularization [24] | 0.490 | 0.740 |
| Random forest [4] | 0.68 | 0.780 |
| Gaussian mixture model [51] | 0.780 | 0.840 |
| Deep learning [28] | 0.650 | 0.880 |
| Active contour and neural networks [52] | 0.863 | 0.887 |
| Proposed method | 0.869 | 0.913 |

their inability to process raw data such as images. In contrast, deformable models take advantage of the features associated with detecting region or edges in the images. The regional characteristics along with the largest gradients can be exploited to find the tumor boundary. The active contour is an example of a deformable model employed for tumor segmentation in this algorithm. The advantages of deformable models like the snake algorithm evidence the powerful achievement of the proposed method.

## 5. CONCLUSION

In this paper, an automated framework was implemented to segment brain tumors in MRI images of high and low-grade gliomas (HGG and LGG). The noticeable high performance and low computational complexity of the algorithm in tumor segmentation confirm the efficiency of the proposed method and suggests a novel combination of active contour and edge sharpening-based image thresholding. Morphological operations were implemented on the binary image to initialize the contour region for use by the snake model. An in-depth analysis was then performed on four well-known edge detection methods to study their effectiveness in image segmentation. The comparison results indicate that Sobel and Canny operators exhibit high performance. The method proposed in this paper outperforms the existing methods using the same MRI images. With its notable performance, the proposed method can support health practitioners in analyzing and diagnosing MRI tumor images, especially those involving a large number of slices.

## REFERENCES

[1] M. Havaei *et al.*, "Brain tumor segmentation with Deep Neural Networks," *Medical Image Analysis*, vol. 35, pp. 18–31, Jan. 2017.

[2] S. Shen, W. Sandham, M. Granat, and A. Sterr, "MRI fuzzy segmentation of brain tissue using neighborhood attraction with neural-network optimization," *IEEE Transactions on Information Technology in Biomedicine*, vol. 9, no. 3, pp. 459–467, Sep. 2005.

[3] Y. Kabir, M. Dojat, B. Scherrer, F. Forbes, and C. Garbay, "Multimodal MRI segmentation of ischemic stroke lesions," in *2007 29th Annual International Conference of the IEEE Engineering in Medicine and Biology Society*, 2007, pp. 1595–1598.

[4] B. H. Menze *et al.*, "The Multimodal Brain Tumor Image Segmentation Benchmark (BRATS)," *IEEE Transactions on Medical Imaging*, vol. 34, no. 10, pp. 1993–2024, Oct. 2015.

[5] N. Gordillo, E. Montseny, and P. Sobrevilla, "State of the art survey on MRI brain tumor segmentation," *Magnetic Resonance Imaging*, vol. 31, no. 8, pp. 1426–1438, Oct. 2013.

[6] J. Kaur, S. Agrawal, and R. Vig, "A comparative analysis of thresholding and edge detection segmentation techniques," *International Journal of Computer Applications*, vol. 39, no. 15, pp. 29–34, 2012.

[7] H. H. Myint and S. L. Aung, "An Efficient Tumor Segmentation of MRI Brain Images Using Thresholding and Morphology Operation," in *Proceedings of the Eighteenth International Conference On Computer Applications (ICCA 2020)*, 2020.

[8] R. G. Selkar and M. N. Thakare, "Brain tumor detection and segmentation by using thresholding and watershed algorithm," *International Journal of Advanced Information and Communication Technology*, vol. 1, no. 3, pp. 321–324, 2014.

[9] K. Thapaliya and G.-R. Kwon, "Extraction of brain tumor based on morphological operations," in *2012 8th International Conference on Computing Technology and Information Management (NCM and ICNIT)*, 2012, pp. 515–520.

[10] Y.-C. Sung, K.-S. Han, C.-J. Song, S.-M. Noh, and J.-W. Park, "Threshold estimation for region segmentation on MR image of brain having the partial volume artifact," in *2000 5th International Conference on Signal Processing & 16th World Computer Congress 2000 (WCC 2000 - ICSP 2000)*, vol. 2, 2000, pp. 1000–1009.

[11] A. Stadlbauer *et al.*,"Improved delineation of brain tumors: an automated method for segmentation based on pathologic changes of 1H-MRSI metabolites in gliomas," *NeuroImage*, vol. 23, no. 2, pp. 454–461, Oct. 2004.

[12] T. Węgliński and A. Fabijańska, "Brain tumor segmentation from MRI data sets using region growing approach," in *Perspective Technologies and Methods in MEMS Design*, 2011, pp. 185–188.

[13] H. Hooda, O. P. Verma and T. Singhal, "Brain tumor segmentation: A performance analysis using K-Means, Fuzzy C-Means and Region growing algorithm," in *2014 IEEE International Conference on Advanced Communications, Control and Computing Technologies*, 2014, pp. 1621–1626.

[14] M. A. Mohammed, M. K. A. Ghani, R. I. Hamed, M. K. Abdullah, and D. A. Ibrahim, "Automatic segmentation and automatic seed point selection of nasopharyngeal carcinoma from microscopy images using region growing based approach," *Journal of Computational Science*, vol. 20, pp. 61–69, May 2017.

[15] A. Mustaqeem, A. Javed, and T. Fatima, "An efficient brain tumor detection algorithm using watershed & thresholding based segmentation,"

*International Journal of Image, Graphics and Signal Processing*, vol. 4, no. 10, pp. 34–39, Sep. 2012.

[16] S. Z. Oo and A. S. Khaing, "Brain tumor detection and segmentation using watershed segmentation and morphological operation," *International Journal of Research in Engineering and Technology*, vol. 3, no. 3, pp. 367–374, Mar. 2014.

[17] S. M. K. Hasan and M. Ahmad, "Two-step verification of brain tumor segmentation using watershed-matching algorithm," *Brain Informatics*, vol. 5, no. 2, 2018, Art. no. 8.

[18] P. Shanthakumar and P. G. Kumar, "Computer aided brain tumor detection system using watershed segmentation techniques," *International Journal of Imaging Systems and Technology*, vol. 25, no. 4, pp. 297–301, Dec. 2015.

[19] C. C. Benson, V. L. Lajish, and K. Rajamani, "Brain tumor extraction from MRI brain images using marker based watershed algorithm," in *2015 International Conference on Advances in Computing, Communications and Informatics (ICACCI)*, 2015, pp. 318–323.

[20] J. Rani, R. Kumar, F. A. Talukdar, and N. Dey, "The Brain Tumor Segmentation Using Fuzzy C-Means Technique: A Study," in *Computer Vision: Concepts, Methodologies, Tools, and Applications*, IGI Global, 2018, pp. 2402–2419.

[21] A. Bal, M. Banerjee, P. Sharma and M. Maitra, "Brain Tumor Segmentation on MR Image Using K-Means and Fuzzy-Possibilistic Clustering," in *2018 2nd International Conference on Electronics, Materials Engineering & Nano-Technology (IEMENTech)*, 2018.

[22] A. Roche, D. Ribes, M. Bach-Cuadra, and G. Krüger, "On the convergence of EM-like algorithms for image segmentation using Markov random fields," *Medical Image Analysis*, vol. 15, no. 6, pp. 830–839, Dec. 2011.

[23] R. Ayachi and N. B. Amor, "Brain tumor segmentation using support vector machines," in *European conference on symbolic and quantitative approaches to reasoning and uncertainty*, 2009, pp. 736–747.

[24] S. Bauer, L.-P. Nolte, and M. Reyes, "Fully automatic segmentation of brain tumor images using support vector machine classification in combination with hierarchical conditional random field regularization," in *International conference on medical image computing and computer-assisted intervention*, 2011, pp. 354–361.

[25] L. P. Clarke, "MR image segmentation using MLM and artificial neural nets," in *American Association of Physicists in Medicine 33rd Annual Meeting and Technical Exhibition*, 1991.

[26] M. Ozkan, B. M. Dawant, and R. J. Maciunas, "Neural-network-based segmentation of multi-modal medical images: a comparative and prospective study," *IEEE Transactions on Medical Imaging*, vol. 12, no. 3, pp. 534–544, Sep. 1993.

[27] A. Işın, C. Direkoğlu, and M. Şah, "Review of MRI-based Brain Tumor Image Segmentation Using Deep Learning Methods," *Procedia Computer Science*, vol. 102, pp. 317–324, 2016.

[28] S. Pereira, A. Pinto, V. Alves, and C. A. Silva, "Brain Tumor Segmentation Using Convolutional Neural Networks in MRI Images," *IEEE Transactions on Medical Imaging*, vol. 35, no. 5, pp. 1240–1251, May 2016.

[29] H. Chen, Z. Qin, Y. Ding, L. Tian, and Z. Qin, "Brain tumor segmentation with deep convolutional symmetric neural network," *Neurocomputing*, vol. 392, pp. 305–313, Jun 2020.

[30] T. Wang, I. Cheng, and A. Basu, "Fluid Vector Flow and Applications in Brain Tumor Segmentation," *IEEE Transactions on Biomedical Engineering*, vol. 56, no. 3, pp. 781–789, Mar. 2009.

[31] J. Sachdeva, V. Kumar, I. Gupta, N. Khandelwal, and C. K. Ahuja, "A novel content-based active contour model for brain tumor segmentation," *Magnetic Resonance Imaging*, vol. 30, no. 5, pp. 694–715, Jun. 2012.

[32] E. Ilunga-Mbuyamba *et al.*, "Localized active contour model with background intensity compensation applied on automatic MR brain tumor segmentation," *Neurocomputing*, vol. 220, pp. 84–97, Jan. 2012.

[33] S. Jiang, Y. Wang, X. Zhou, Z. Chen, and S. Yang, "Brain Extraction Using Active Contour Neighborhood-Based Graph Cuts Model," *Symmetry*, vol. 12, no. 4, 2020, Art. no. 559.

[34] Y. Li, G. Cao, T. Wang, Q. Cui, and B. Wang, "A novel local region-based active contour model for image segmentation using Bayes theorem," *Information Sciences*, vol. 506, pp. 443–456, Jan. 2020.

[35] C.-C. Chang, J.-Y. Hsiao, and C.-P. Hsieh, "An adaptive median filter for image denoising," in *2008 Second International Symposium on Intelligent Information Technology Application*, vol. 2, 2008, pp. 346–350.

[36] N. Nausheen, A. Seal, P. Khanna, and S. Halder, "A FPGA based implementation of Sobel edge detection," *Microprocessors and Microsystems*, vol. 56, pp. 84–91, Feb. 2018.

[37] G. T. Shrivakshan and C. Chandrasekar, "A comparison of various edge detection techniques used in image processing," *International Journal of Computer Science Issues*, vol. 9, no. 5, pp. 269–276, Sep. 2012.

[38] G. N. Chaple, R. D. Daruwala, and M. S. Gofaneh, "Comparisions of Robert, Prewitt, Sobel operator based edge detection methods for

real time uses on FPGA," in *2015 International Conference on Technologies for Sustainable Development (ICTSD)*, 2015.

[39] S. S. Al-Amri, N. V Kalyankar, and S. D. Khamitkar, "Image segmentation by using edge detection," *International Journal on Computer Science and Engineering*, vol. 2, no. 3, pp. 804–807, May 2010.

[40] S. S. Al-Amri, N. V Kalyankar, and S. D. Khamitkar, "Image segmentation by using threshold techniques," *Journal of Computing*, vol. 2, no. 5, pp. 83–86, May 2010.

[41] R. C. Gonzalez and R. E. Woods, *Digital Image Processing*, 4th ed. Upper Saddle River, NJ, USA: Pearson, 2018.

[42] M. S. H. Al-Tamimi and G. Sulong, "A Review of Snake Models in Medical MR Image Segmentation," *Jurnal Teknologi*, vol. 69, no. 2, pp. 101–106, Jun. 2014.

[43] N. Nabizadeh, "Automated Brain Lesion Detection and Segmentation Using Magnetic Resonance Images," Ph.D. dissertation, University of Miami, Coral Gables, FL, USA, 2015.

[44] M. Kass, A. Witkin, and D. Terzopoulos, "Snakes: Active contour models," *International Journal of Computer Vision*, vol. 1, no. 4, pp. 321–331, Jan. 1988.

[45] R. J. Hemalatha, T. R. Thamizhvani, A. J. A. Dhivya, J. E. Joseph, B. Babu, and R. Chandrasekaran, "Active Contour Based Segmentation Techniques for Medical Image Analysis," in *Medical and Biological Image Analysis*, R. Koprowski, Ed. IntechOpen, 2018.

[46] N. Nabizadeh and M. Kubat, "Brain tumors detection and segmentation in MR images: Gabor wavelet vs. statistical features," *Computers & Electrical Engineering*, vol. 45, pp. 286–301, Jul. 2015.

[47] J. Bertels *et al.*, "Optimizing the Dice Score and Jaccard Index for Medical Image Segmentation: Theory and Practice," in *International Conference on Medical Image Computing and Computer-Assisted Intervention – MICCAI 2019* (Lecture Notes in Computer Science, vol. 11765), D. Shen *et al.*, Eds. Cham, Switzerland: Springer Nature, 2019, pp. 92–100.

[48] G. Csurka, D. Larlus, F. Perronnin, and F. Meylan, "What is a good evaluation measure for semantic segmentation?," in *Proceedings of the British Machine Vision Conference 2013*, 2013, pp. 32.1–32.11.

[49] M. U. Akram and A. Usman, "Computer aided system for brain tumor detection and segmentation," in *International Conference on Computer Networks and Information Technology*, 2011, pp. 299–302.

[50] S. B. Kumar, R. Panda, and S. Agrawal, "Brain Magnetic Resonance Image Tumor Detection and Segmentation Using Edgeless Active Contour," in *2020 11th International Conference on Computing, Communication and Networking Technologies (ICCCNT)*, 2020.

[51] L. Zhao, D. Sarikaya, and J. J. Corso, "Automatic Brain Tumor Segmentation with MRF on Supervoxels," in *Proceedings of NCI-MICCAI Challenge on Multimodal Brain Tumor Segmentation (NCI-MICCAI BRATS 2013)*, Nagoya, Japan, Sep. 22, 2013, pp. 51–54.

[52] M. Soleymanifard and M. Hamghalam, "Segmentation of Whole Tumor Using Localized Active Contour and Trained Neural Network in Boundaries," in *2019 5th Conference on Knowledge Based Engineering and Innovation (KBEI)*, 2019, pp. 739–744.

**Mustafa Rashid Ismael** received his B.S. degrees in electrical engineering from the University of Babylon, Babel, Iraq, in 2004, M.S. degree in electronic engineering from the University of Technology, Baghdad, Iraq, in 2011, and Ph.D. degree in electrical and computer engineering from Western Michigan University, Kalamazoo, MI, USA, in 2018. He is currently working as an assistant professor at the Department of Electrical Engineering, University of Babylon, Babel, Iraq. His research interest includes image processing, pattern recognition, feature extraction, cognitive radio, and other signal processing problems.